

# Soft x-ray interferometry for pump-probe spectroscopy and hyperspectral imaging

Contact [k.okeeffe@stfc.ac.uk](mailto:k.okeeffe@stfc.ac.uk)

**K. O’Keeffe**

College of Science, Department of Physics, Swansea University  
Swansea, United Kingdom,

**D. T. Lloyd**

Department of Physics, University of Oxford  
Oxford, United Kingdom

**A. S. Wyatt, R. Chapman, C. Thornton, P. Majchrzak, A. Jones, E. Springate**

Central laser Facility, STFC Rutherford Appleton Laboratory  
Harwell, United Kingdom

## Introduction

The ability to probe matter at high temporal and spatial resolutions is crucial to our understanding of many fundamental processes in nature. The creation of soft x-ray pulses at femtosecond and attosecond timescales via high-harmonic generation (HHG) has enabled a host of seminal works such as the observation of ultrafast dynamics in gases [1], and solids [2]. The fundamental physics of HHG is well described by the semi-classical three-step model [3]. In this model electrons generated via tunnel ionization in the presence of a strong laser field are acceleration back towards their parent ion where they can recombine, with the emission of harmonic photons at odd integer multiples of the fundamental driving frequency. In this process the maximum harmonic photon which is generated is proportional to the peak laser intensity. For harmonics generated below the maximum photon energy electrons can return to their parent ion with the same kinetic energy via two predominant paths. These paths are known as the “long” and “short” quantum trajectories, in reference to the different times an electron spends in the continuum, with the long trajectory taking up to almost a full optical cycle for an electron to return to its parent ion.

The phase of the generated harmonics depends sensitively both on the quantum trajectory and the intensity of the driving laser pulse, resulting in the emission of radiation which exhibits strong space-time coupling. Precise characterization of the phase contribution to the harmonic field arising from quantum paths is therefore key to fully exploiting the space-time properties of the emitted attosecond extreme ultraviolet radiation, as well as providing new insights into the ultrafast dynamics of the emitting species. Reported here is a new technique for identifying the contributions of the different quantum trajectories present in HHG.

It has recently been demonstrated that by analyzing the spatially-resolved harmonic spectrum as a function of the longitudinal separation between two HHG sources driven sequentially by the same laser pulse, trajectory-dependent interference can be identified [4]. The origins of this interference lie in the difference between the geometric and atomic phase shifts experienced by each source within the focal region. The on-axis phase of harmonics generated in each source about the focal region is given approximately by  $\phi_q = q\phi_G + \phi_{at}$  where  $q$  is the harmonic order,  $\phi_G$  is the Gouy phase, and  $\phi_{at}$  is the atomic dipole phase. The Gouy phase is approximately linear within the focal region and imparts a delay between the longitudinally separated harmonic sources which can be controlled with zeptosecond stability [5]. The atomic dipole phase  $\phi_{at} \approx -\alpha I(r, z)$  accounts for the phase accumulated by electrons during the HHG process, and is different for long and short trajectories through the parameter  $\alpha$ , which depends on the transit time of electrons in the continuum. Since the laser intensity,  $I(r, z)$ , and therefore  $\phi_{at}$ , varies with transverse position,  $r$ , as well as with longitudinal position in the focus,  $z$ , the far-field distribution from two longitudinally separated sources exhibits interference effects in both  $r$  and  $z$ ,

with trajectory-specific interference contained in the  $r$ -domain. In this work we expand on the technique demonstrated in [4] to show that by increasing the dimensionality of such an inline interferometer it is possible to distinguish the contributions of the long and short quantum paths in the resulting HHG interferograms.

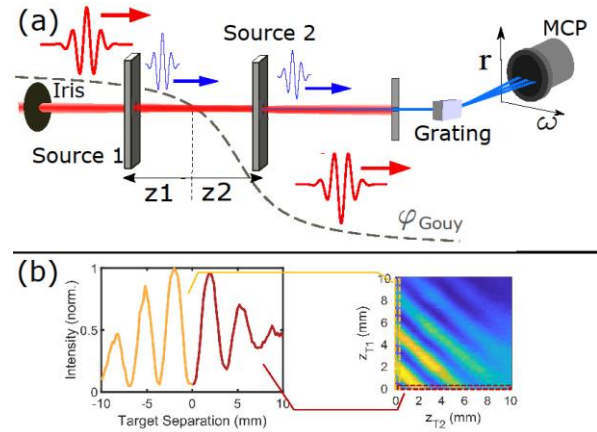


**Figure 1:** (a) Experimental setup. The spatially-resolved harmonic spectrum generated from two longitudinally separated gas targets is recorded as a function of the positions ( $z_1, z_2$ ) of each gas cell. The Gouy phase shift across the focus and variation in the atomic dipole phase results in interference between the harmonics generated in each target. (b) Left: the on-axis harmonic interference resulting from moving a single cell about the focus while keeping the other static. Right: On-axis interferogram for  $q=15$  resulting from moving both cells about the focus.

## Experiment

A schematic of the experiment is shown in Figure 1 (a). Two thin gas cells, each formed of a hollow, nickel tube, pressed to an outer thickness of 0.6 mm, were placed within the focus of a driving laser beam and backed with argon. The gas cell lengths were much smaller than the Rayleigh range of the focused beam and low gas pressures ( $<10$ mbar) are used in each cell such that propagation effects including phase-matching and absorption are minimized. Each gas cell could be moved independently within the laser focus. A 780 nm laser was used to generate harmonics and the spatially-resolved high-harmonic spectrum was recorded as a function of the longitudinal position of both gas cells, using a flat-field extreme ultraviolet spectrometer. The pressure in each gas cell could be controlled independently, and was adjusted to achieve equal harmonic intensities from each cell individually, such that the interferometer was balanced. A single scan involved measuring the harmonic intensity as a function of four parameters: harmonic frequency ( $\omega_q$ ), radial position on the spectrometer  $R$ , position of the first gas cell ( $z_1$ ), and position of the second cell ( $z_2$ ). This corresponds to recording an interferogram in the  $(\omega_q, R, z_1, z_2)$

domain. A subset of such an interferogram is shown in Figure 1 (b), corresponding to  $(z_1, z_2)$  interference of the on-axis ( $R=0$ ) component for  $q = 15$ . As can be seen in Figure 1 (b) strong modulation in the on-axis harmonic intensity are observed as a function of the position of both targets within the focal region.

However, the measured interferograms vary significantly in the radial dimension. This is due to the transverse dependence of the atomic dipole phase, which varies differently for the long and short trajectory components for each harmonic below the maximum photon energy. Analyzing the radial dependence of the interferograms for a particular harmonic order should therefore yield information on the contribution of the different electron trajectories to the resulting interference patterns. In order to understand the evolution of these fringe patterns an analytic model of the harmonic generation in both cells was developed, similar to that described in [6]. The field from each HHG source were calculated and propagated to the detector plane using the Hankel transform after which the interference patterns at various divergence angles were evaluated. Figure 2 compares the experimental interferograms at different divergence angles with the simulated interference patterns.

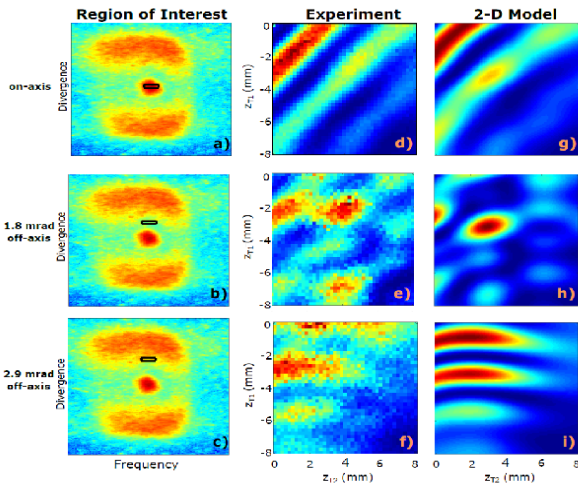


**Figure 2.** Left column: Spatio-spectral profile recorded for harmonic order  $q=15$ . The black box indicated the region of interest at which the interferogram is analysed with a) on-axis, b) 1.8mrad off-axis, and c) 2.9mrad off-axis. Middle column: d), e), and f) show the measured interference patterns at the regions of interest highlighted in a), b), and c), respectively. Right column: g), h), and i) show the simulated interference patterns at the regions of interest shown in a), b) and c).

The on-axis interference observed in Figure 2 is dominated by the short trajectory contribution from each harmonic source as this has a low divergence angle, whereas in the far off-axis region the interference is dominated by the long-trajectory component from each source. At intermediate divergence angles the long and short trajectory components can have equal weights giving rise to the complex interference patterns observed in Figure 2 e) and h). The fringe pattern in this regime is sensitive to the relative phase between the two trajectories, providing insight into the timing between the long and short trajectory components.

The performance of the interferometer was investigated for a wide range of experimental parameters, including using long-wavelength fundamental driving fields, different gas species in each cell, and elliptically polarized laser fields. Interference was observed for a wide range of experimental parameters investigated, demonstrating the robustness of this technique. In particular, clear species-dependent phase shifts were observed in the measured interference patterns arising from HHG from

different gas species. Analysis of the phase shifts in these interference patterns may provide new insight into electron-ion recollisions during the HHG process.

## Conclusion

We have demonstrated an inline HHG interferometer which grants experimental access to the relative weight and phase-shifts present in harmonic emission. The high timing stability inherent in this setup, together with its sensitivity to the quantum trajectories present in HHG, may provide a new approach for probing ultrafast processes in complex molecular systems.

## References

1. J. C. Peterson *et al.*; Physics Review Letters, **107**, 177402 (2011)
2. E. Goulielmakis *et al.*; Nature (2010)
3. P. Corkum *et al.*; Physical Review Letters, **71**, 1994, (1993)
4. M. M. Mang *et al.*; Optics Letters, **43**, 5275, (2018)
5. D.E. Laban *et al.*; Physical Review Letters, **26**, 109, (2012)
6. F. Catoire *et al.*; Physical Review A, 94, 063401, (2016)